J. Braz. Chem. Soc., Vol. 18, No. 8, 1515-1523, 2007.
Printed in Brazil - ©2007 Sociedade Brasileira de Química
0103 - 5053 $6.00+0.00

Article

Natural Polyprenylated Benzophenones: Keto-Enol Tautomerism and Stereochemistry

Felipe T. Martins,[a] José W. Cruz Jr.,[a] Priscilla B. M. C. Derogis,[b] Marcelo H. dos Santos,[b] Márcia P. Veloso,[b] Javier Ellena[c] and Antônio C. Doriguetto*[,a]

[a]Laboratório de Cristalografia and [b]Laboratório de Fitoquímica e Química Medicinal, Departamento de Ciências Exatas, Universidade Federal de Alfenas, 37130-000 Alfenas-MG, Brazil

[c]Instituto de Física de São Carlos, Universidade de São Paulo, CP 369, 13560-970 São Carlos-SP, Brazil

O estudo do tautomerismo ceto-enólico e da estereoquímica de uma benzofenona natural com propriedades inibitórias sobre HIV, denominada (1*R*,5*R*,7*R*,8*S*)-(+)-3-(10-(3,4-diidroxifenil)-10-hidroximetileno)-8-metil-1,5,7-tris(3-metil-2-butenil)-8-(4-metil-3-pentenil)-biciclo[3.3.1]nonano-2,4,9-triona (**a**), a qual foi isolada das sementes de *Garcinia brasiliensis*, é apresentado. A estrutura cristalina de (**a**), também conhecida como gutiferona A, foi determinada por difração de raios X e suas geometrias intra e intermolecular discutidas e comparadas com duas benzofenonas naturais análogas: clusianona and epiclusianona. Em (**a**), o átomo de hidrogênio hidroxílico proveniente do sistema ceto-enólico 2,4,10-triona está ligado ao átomo de oxigênio conectado ao grupo 10-(3,4-diidroxifenil)metileno, contrariamente ao verificado nas outras duas benzofenonas naturais similares, onde o átomo de hidrogênio equivalente está ligado em diferentes átomos de oxigênio pertencentes ao sistema anelar biciclo[3.3.1]nonano. Tal comportamento pode ser explicado pela presença do grupo OH6 no anel aromático que origina uma via ressonante deslocalizada adicional ao longo do sistema 3,4-diidroxifenil-C10-OH2. Em adição, a estereoquímica em torno do átomo C7 de (**a**) é comparada com as estruturas conhecidas da clusianona e da epiclusianona e a influência da configuração neste átomo de carbono quiral sobre as características estruturais encontradas no sistema ceto-enólico é proposta.

The keto-enol tautomerism and stereochemistry study of a HIV-inhibitory natural benzophenone, (1*R*,5*R*,7*R*,8*S*)-(+)-3-(10-(3,4-dihydroxyphenyl)-10-hydroxymethylene)-8-methyl-1,5,7-tris(3-methyl-2-butenyl)-8-(4-methyl-3-pentenyl)-bicyclo[3.3.1]nonane-2,4,9-trione (**a**), isolated from *Garcinia brasiliensis* seeds is presented. The crystal structure of (**a**), which is also know as guttiferona A, was determined by X-ray diffraction and its intra and inter-molecular geometries discussed and compared with two analogue natural benzophenones: clusianone and epiclusianone. In (**a**), the hydroxyl H atom from enolizable 2,4,10-trione moiety is linked in the oxygen atom bonded to 10-(3,4-dihydroxyphenyl)methylene group, in opposition to the related natural benzophenones, where this analogue H-atom is placed in different O-atoms from bicyclo[3.3.1]nonane ring system. Such behaviour can be explained by the presence of aromatic OH6 group in (**a**) that origins a further delocalized resonance path along of 3,4-dihydroxyphenyl-C10-OH2 group. In addition, the (**a**) stereochemistry around C7 atom is compared with known structures of clusianone and epiclusianone and the influence from configuration in this chiral C-atom to structural features found in the enolizable system is proposed.

Keywords: guttiferone A, keto-enol tautomerism, benzophenone, X-ray diffraction, stereochemistry

Introduction

The Guttiferae family presents a variety of biologically active metabolites, such as polyisoprenylated benzophenones.[1,2] Several HIV-inhibitory prenylated benzophenones derivatives, named guttiferones, were previously isolated from extracts of Guttiferae species, mainly of three different genera (*Garcinia, Clusia* and *Symphonia*). The wide spectrum of biological activities of these compounds include the cytophatic effects inhibiting

*e-mail: doriguetto@unifal-mg.edu.br

of *in vitro* HIV infection;[1] free radical scavenging; iNOS and COX-2 expression inhibiting in colon carcinoma; apoptosis induction and antiulcer, antioxidant and trypanocidal properties.[3-7]

Garcinia or *Rheedia* is the most numerous genus of the Guttiferae family with about 400 species widely distributed in tropical Asia, Africa, New Caledonia, Polynesia and Brazil.[8] This genus is widely used in the Brazilian popular medicine and it is known to be rich in oxygenated and prenylated phenol derivatives,[9,10] including the polyisoprenylated benzophenones.[11] Some of them present various biological activities, such as anti-inflammatory,[12] antitumoral[13] and antioxidant properties.[14]

The (1*R*,5*R*,7*R*,8*S*)-(+)-3-(10-(3,4-dihydroxyphenyl)-10-hydroxymethylene)-8-methyl-1,5,7-tris(3-methyl-2-butenyl)-8-(4-methyl-3-pentenyl)-bicyclo[3.3.1]nonane-2,4,9-trione (**a**), usually named of guttiferone A, was initially isolated from *Symphonia globulifera* as an active anti-HIV compound.[1] This compound was also isolated from *Garcinia intermedia*.[3] The chemical structure in the solid state of epiclusianone, a benzophenone purified from *Garcinia gardneriana* fruit peel extracts that also presents interesting biological actions as vascular effects on the rat aorta[15] and anti-HIV activity,[16] was previously determined through X-ray diffraction analysis by our research group.[17] We here discussed the crystalline structure of the (**a**), a benzophenone extracted and purified from seeds of *Garcinia brasiliensis* (Mart.) Planch. & Triana, a *Garcinia* specie largely found in Brazil. The structural features of (**a**) were compared with that from related benzophenones clusianone and epiclusianone, taking into account the substitution pattern in (**a**) and the stereochemistry around C7 atom.

Experimental

Plant material and preparation of extract

The fruits of *G. brasiliensis* were collected in the *Campus* of Universidade Federal de Viçosa (UFV), Viçosa, Brazil, and identified by a botanist of UFV. The voucher specimen is deposited in Horto Botânico of UFV (register number VIC26240).

The dried and powdered fruit seeds of *G. brasiliensis* (700 g) were macerated at room temperature with 3.0 L of ethanol:water (95:5, v/v). The resulting mixture was filtered and then dried using a rotary evaporator under reduced pressure at 45 °C. These procedures were repeated by five times when residues were gotten yielding 80 g of ethanolic extract from *G. brasiliensis* seeds (EES).

*Isolation of (**a**)*

The EES was chromatographed on a silica gel (230-400 mesh) column (8 x 100 cm) eluted with crescent polarity mixtures of *n*-hexane/ethyl-acetate and ethyl-acetate/ethanol to give fifty fractions of 250 mL each one that had been rejoined in four groups for similarity in TLC (thin layer chromatography): EES-1 (frs-1-6, 9.5 g, a mixture of fat acids esters), EES-2 (frs-4-20, 1.9 g, resinous orange material), EES-3 (frs-21-33, a yellow solid) and EES-4 (frs-34-50, 2.6 g, a complex mixture of polar compounds). EES-3 (5.0 g) was washed with acetone obtaining two portions: the insoluble portion (EES-3I) containing 1.0 g of a hydrocarbons mixture, and the soluble portion (EES-3S, 1.5 g). The EES-3S fraction was recrystallized several times with methanol solution to afford the (**a**) (0.5 g) as yellow crystalline solid.

Single crystal X-ray diffraction

After the isolation and purification of compound (**a**), a well-shaped clear single crystal was selected for the X-ray diffraction experiment. Intensity data were measured with the crystal at room temperature (293 K) and with graphite monochromated MoKα radiation (λ = 0.71073 Å), using the *Enraf-Nonius Kappa-CCD* diffractometer. The cell refinements were performed using the software Collect[18] and Scalepack,[19] and the final cell parameters were obtained on all reflections. Data for (**a**) were measured up to 50.75° in 2θ, totaling 27682 Bragg reflections. Data reduction was carried out using the software Denzo-SMN and Scalepack[19] and XdisplayF for visual representation of data. No significant absorption coefficient of 0.075 mm^{-1} was observed for (**a**). So, no absorption correction was applied.

The structure was solved using the software SHELXS-97[20] and refined using the software SHELXL-97.[21] C and O atoms of the molecules were clearly solved and full-matrix least-squares refinement of these atoms with anisotropic thermal parameters was carried on. The C-H hydrogen atoms were positioned stereochemically and were refined with fixed individual displacement parameters [$U_{iso}(H) = 1.2U_{eq}(C_{sp^2})$ or $1.5U_{eq}(C_{sp^3})$] using a riding model with aromatic C—H bond length of 0.93 Å, methyl C—H one of 0.96 Å, methylene C—H one of 0.97 Å and methine C—H one of 0.98 Å. The hydroxyl H atoms were located by difference Fourier synthesis and were set as isotropic. Maps of residual electronic density were obtained

by difference Fourier synthesis in order to show the localization of the remaining H-atom in (**a**) and in epiclusianone. For this purpose, the positional parameter of this H-atom was not constrained during refinements. In the case of epiclusianone, the experimental data used in difference Fourier synthesis had been collected earlier by one of us.[17] Crystal, collection and structure refinement data are summarized in Table 1.

Tables were generated by WinGX,[22] and others softwares were also used in order to publish the crystal data, as ORTEP-3[23] and MERCURY.[24] The molecular conformation and geometry were studied through MOGUL,[25] a knowledge base that take a molecule submitted either manually or by another computer program via an instruction-file interface and perform substructure searches of the Cambridge Structural Database (CSD)[26] for, typically, all its bonds, angles, and torsional angles.

In spite of (**a**) crystallizing in a non-centrosymmetric space group, the Flack parameter was not refined during X-ray crystallographic analysis. Since the most electron-rich atom is oxygen, which does not have an anomalous scattering large enough (using MoK_{α} radiation) to permit determination of the absolute structure using X-ray diffraction, Friedel pairs were averaged before refinement.

Spectroscopic measures and instrumentation general methods

UV spectrum was determined on Shimadzu U-2000 spectrophotometer. Infrared spectrum was obtained using KBr discs in a Shimadzu/IR-408 spectrophotometer; ^{1}H and ^{13}C NMR spectrum (in pyridine-d_5) was run on a Bruker spectrometer equipped with a 5 mL ^{1}H and ^{13}C probe operating at 400.1 and 100.6 MHz, respectively, with TMS as internal standard. Mass spectrum was obtained from a gas chromatography-mass spectrometry (GC-MS) using a Shimadzu GCMS QP5050A equipment connected to an ion trap detector operating in Electron Impact mode at 70 eV, with a sampling rate of 0.50 scans/s and scanning speed of 1000. Melting point was determined on Mettler melting point apparatus FP 80 HT. Optical rotation was carried out on Perkin-Elmer-241 spectrophotometer.

Results and Discussion

Figure 1a is an ORTEP-3[23] view of the (**a**), and the crystal, collection and structure refinement data are displayed in Table 1. The stereochemistry around C7 atom is the same in (**a**) and in another natural benzophenone, epiclusianone (Figure 1b), showing that absolute configuration of (**a**) is related to that established in such natural benzophenone. Either in (**a**) or epiclusianone, the prenyl group including from C24 to C28 atoms is above the plane passing through atoms C1, C5 and C7, in an axial orientation (Figure 2). Another similarity between these two substances is in the rotation of the aromatic head around the C3-C10 bond axis, which is identical in both structures in reason of the molecular stabilization to occur by H-bond involving the O1 and O2 atoms (Figure 2). On the other hand, in the epimer of epiclusianone, clusianone, it is observed that the benzoyl group is rotated about 180° around C3-C10 axis in comparison with epiclusianone and (**a**). This fact is consequence of the H-bond in query to be located between the O2 and O3 atoms in clusianone, differently from epiclusianone and (**a**). In clusianone, the configuration in the C7 atom states that C24-C28 prenyl group is below C1-C5-C7 plane, in an equatorial orientation.[27] The explanation for this differential H-bond localization can be in the stereochemistry of C7 atom. In the cases of epiclusianone and (**a**), the axial position of prenyl group approximates the C25=C26 and C2=O3 groups (Figure 2), favoring an intramolecular dipolar interaction between such ones.[28] The intramolecular distances from the centroid calculated between C25 and C26 atoms to the O3 atom are 3.734(4) Å in epiclusianone and 3.698(2) Å in (**a**). Such distances are very similar in both compounds, as well as they are also suitable to occurrence of the intramolecular contact above mentioned.[29] Due to possible dipolar contact, the C2=O3 carbonyl group acting as electronic donor to C25=C26 group remains with electronic deficiency, which hinders the covalent O3-H2 H-bond in the case of epiclusianone and the intramolecular O2-H2…O3 H-bond in the case of (**a**). In this way, the intramolecular H-bond is formed between O1 and O2 atoms as reported in epiclusianone and (**a**). For clusianone, the equatorial position of prenyl group increases the distance between the C25=C26 and C2=O3 groups to 5.321 Å. So, the intramolecular contact cited in epiclusianone and (**a**) is unavailable in clusianone, and the electronic deficiency is not achieved in C2=O3 group. As result, the O3 atom bonds covalently to H2 atom and the benzoyl group rotates 180° in order to stabilize the structure via O3-H2…O2 H bond, as described by McCandlish *et al.*[27]

Selected bond lengths and angles of (**a**) are available in supplementary material. The intra-molecular geometry of (**a**) was analyzed using MOGUL,[25] a knowledge base of molecular geometry derived from Cambridge Structural Database CSD,[26] that provides access to information on the preferred values of bond lengths, valence angles and acyclic torsion angles. This study showed that all bond

lengths and bond angles are in agreement with the expected values for a good X-ray diffraction structure refinement. However, the MOGUL analysis has pointed out interesting geometrical features due to resonance highlighting that this X-ray crystallography knowledge base is a powerful tool to clarify structural relationships in chemical compounds. Using such method we observed variations in (**a**) that show clearly the electronic delocalization at a conjugated system characterized by keto-enol tautomerism, as well as the influence of aromatic hydroxyl groups to the intra-molecular crystal structure.

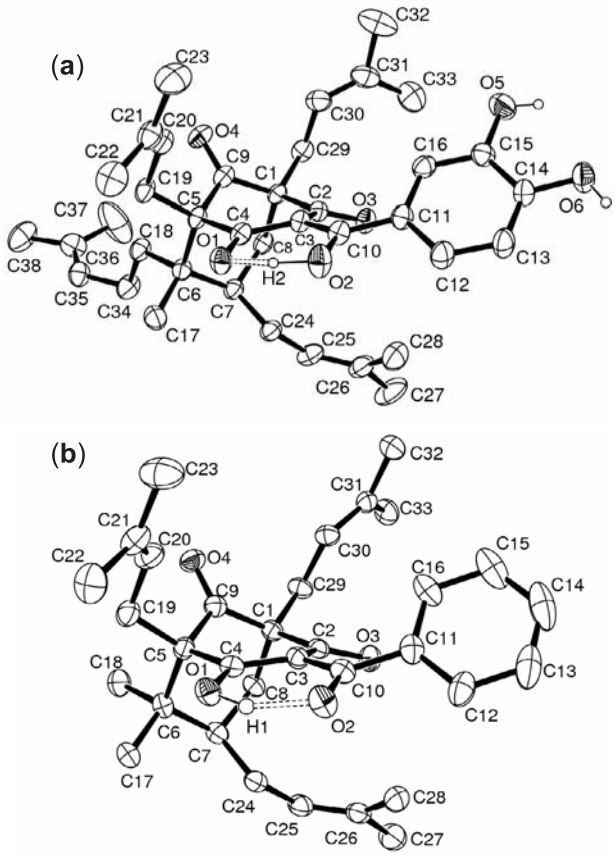

Figure 1. (a) ORTEP view of (**a**) showing the arbitrary atom labeling. Ellipsoids represent 50% probability level. Double dotted lines represent hydrogen bonds. The C-H H atoms were omitted for clarity. (b) The ORTEP view of epiclusianone[17] is shown in the same conditions.

It was observed that the double bonds C3=C10 (1.413(5) Å) and O1=C4 (1.281(4) Å) are markedly longer than the average query values, whereas the single bonds C3-C4 (1.416(5) Å) and O2-C10 (1.297(5) Å) are shorter than the expected ones. These features are consequence of entire electronic delocalization through the atoms O2-C10-C3-C4-O1 that in solution lead to distinct tautomeric forms.[1,2,30] However, in the (**a**) crystal structure the model considering the C10-OH2 tautomer gives the best fitted final refinement indexes. In this way, from a statistical

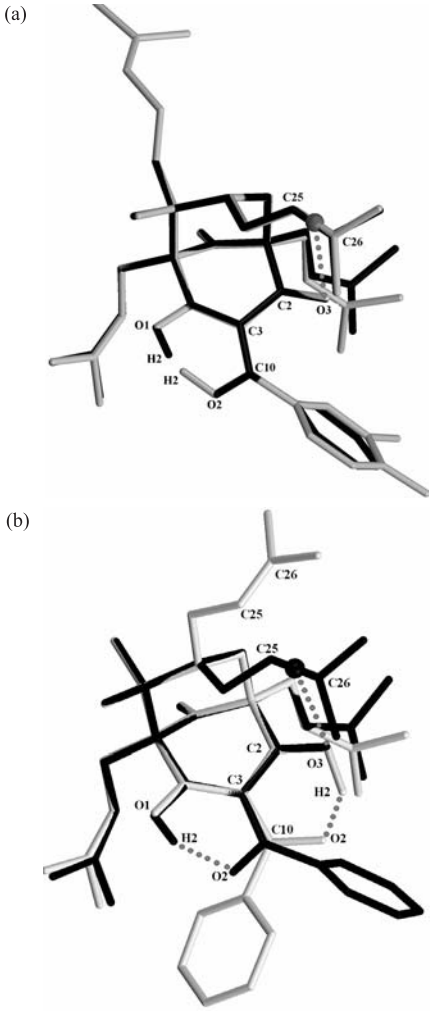

Figure 2. Structure views showing the superposition of a) guttiferone A (dark grey) and epiclusianone (black) substances; and b) epiclusianone (black) and clusianone (light grey) ones. The centroids (balls) were calculated between C25 and C26 atoms from (**a**) and epiclusianone in Figures 2a and 2b, respectively. The dotted lines represent the intramolecular H-bonds and the distances from centroids to the O3 atom. The OH and H atoms from keto-enol moiety were displayed.

point of view revelled by XRD analysis, this model must be taken in account in the moment of structural assignments by NMR spectroscopic techniques performed in solution.

Opposed behaviours were previously reported in crystal structures of clusianone[27] and epiclusianone,[17] two related polyprenylated benzophenones presenting the same moiety involved in the tautomerism, where the tautomers that presented the highest relative contribution to hybrid structure were the C10=O2/C2-O3-H2 and C10=O2/C4-O1-H2 forms, respectively. Comparing the lengths of bonds into delocalized system, it was possible to find crucial differences between (**a**) and clusianone/epiclusianone. The lengths of the bonds equivalent to (**a**) C3=C10, O3=C2, C2-C3 and O2-C10 are respectively 1.448, 1.304, 1.388

Table 1. Crystal data and structure refinement for (**a**)

	guttiferone A
Empirical formula	$C_{38}H_{50}O_6$
Formula weight	602.78
Temperature / K	293(2)
Wavelength / Å	0.71073
Crystal system	Orthorhombic
Space group	$P2_12_12_1$
Unit cell dimensions	a =8.8660(4) Å
	b=11.5210(5) Å
	c=34.4940(16) Å
Volume / Å^3	3523.4(3)
Z	4
Density (calculated) / (mg m^{-3})	1.136
Absorption coefficient / mm^{-1}	0.075
F(000)	1304
Crystal size / mm	0.35 × 0.07 × 0.06
θ-Range for data collection / (°)	2.95-25.37
Index ranges	$-10 \le h \le 10$; $-13 \le k \le 13$; $-41 \le l \le 40$
Reflections collected	27682
Independent reflections	3650 [R(int) = 0.0672]
Completeness to θ =25.37°	99.3 %
Refinement method	Full-matrix least-squares on F^2
Data/restraints/parameters	3650 / 0 / 401
Goodness-of-fit on F^2	1.024
Final R for $I > 2\sigma(I)$	$R1$=0.0536
R indices (all data)	$wR2$=0.1538
Largest diff. peak and hole / (e.Å^{-3})	0. 172, -0.186

and 1.266 Å in clusianone,[27] and those equivalent to (**a**) C3=C10, O1=C4, C3-C4 and O2-C10 are respectively 1.449(6), 1.299(6), 1.380(6) and 1.268(6) Å in epiclusianone.[17] Considering the first two bonds, C3=C10 and O3=C2 for clusianone and C3=C10 and O1=C4 for epiclusianone, the values of lengths have increased 0.05(1) and 0.02(1) Å, respectively, in comparison with the respective ones determined for (**a**), whereas the last two bond distances, C2-C3 and O2-C10 for clusianone and C3-C4 and O2-C10 for epiclusianone, have respectively decreased 0.05(2) and 0.03(2) Å when compared with the bond lengths equivalent in (**a**). Indeed, theses differences above mentioned just confirm the presence, in the solid state, of distinct structural forms with regard to keto-enol tautomeric moiety from (**a**), clusianone and epiclusianone. One suitable explanation for this tautomeric varying between (**a**) and clusianone/epiclusianone in crystal structures can be extracted analyzing the C10-C11 bond. This bond length is 1.469(6) Å in (**a**), whereas these values in clusianone and epimer are 1.489 and 1.482(7) Å, respectively. So, the highlighted shortening of (**a**) C10-C11 bond can be interpreted as a character of double bond and is quite probable to be a consequence of O6-H6 group in *para*-position from aromatic ring. This hydroxyl group, an electron-donating ring substituent, origins a delocalized resonance path passing through atoms OH6-Ph-C11-C10-O2 that increases the electronic density around O2 atom. Thus, the OH covalent bonding occurs on the O2 atom instead of the O1 atom, as in epiclusianone, or on the O3 atom, as in clusianone. In this way, C4=O1 and C2=O3 remain as carbonyl groups in (**a**). The bond distances O2-H2 (1.04(6) Å) and H2...O1 (1.41(5) Å) state clearly the observation above mentioned. The Figure 3 is a map of residual electronic density obtained by difference Fourier synthesis that was used to localise the remaining H atom in (**a**) and epiclusianone. Since the most electron-rich atom is oxygen, which allow a suitable localization of hydrogen atoms in small molecules, Figure 3 shows that hydrogen atoms are linked covalently to O2 in (**a**) and to O1 in epiclusianone in agreement with the intra-molecular features above detailed.

To strengthen the structural relationships about the differential tautomeric contribution in (**a**) and epiclusianone, we also analyzed another intra-molecular feature: the torsional angle between C10-O2 group and the least squares plane through aromatic ring. For (**a**) is observed a torsional angle of 31.1(5)° for C12-C11-C10-O2, whereas in epiclusianone this value is 37.3(7)°. This slight decreased twisting in (**a**) can be viewed as consequence of additional electronic conjugation offered by 3,4-dihydroxyphenyl group in resonance with C10-O2 one, which give subtle rise to planarity between the query

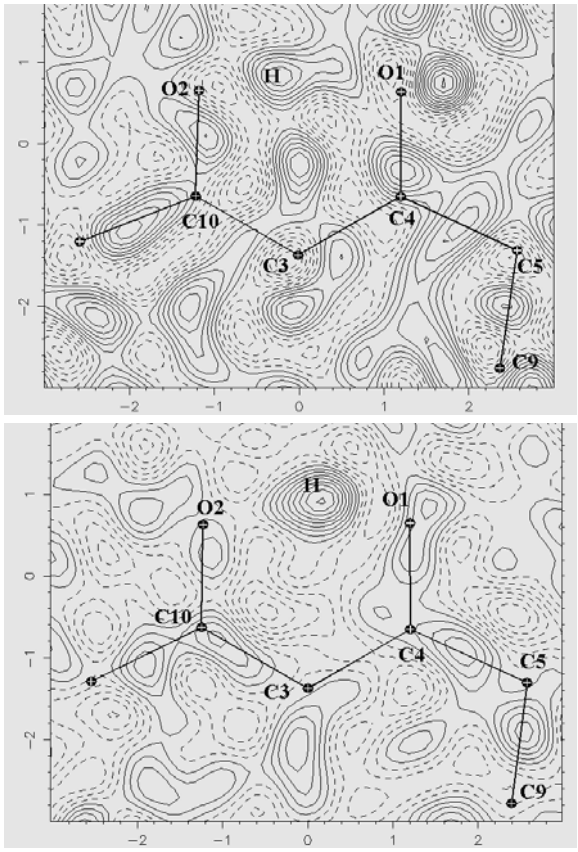

Figure 3. Residual density map of keto-enol moiety from (**a**) and epiclusianone, obtained by difference Fourier synthesis. Solid lines show positive contours and dotted lines show the negative contours. Contour levels are 0.026 $e.Å^{-3}$ intervals.

groups. However, such planarity is not so increased due to the presence of the strong intramolecular hydrogen bond O2-H2…O1 that leads to chelating hexacyclic system formed by O2-C10-C3-C4-O1-H2 atoms. The highest deviation from the least squares plane passing through the six cyclic atoms above mentioned is -0.046(3) Å for H2, showing that such system is practically planar. Furthermore, the O1…O2 separation is 2.390(4) Å, having an angle of 155(5)° between O2-H2…O1, being that such distance between the O-atoms is slightly shorter than that found in similar benzophenones as clusianone (2.418 Å)[27] and epiclusianone (2.430(4) Å).[17] The strong intramolecular H-bond O2-H2...O1 can also explain significant valence angles deviances. All angle deviations that will be below mentioned can be view as result of one primary enlargement at the C3-C4-C5 angle where the carbonylic O1 atom is bonded. This angle (123.29(3)°) in (**a**) is significantly increased in comparison with average angles whose the corner C atom is carbonylic (118(3)°). In turn, several adjacent angles are contracted and others expanded as presumed. For instance, the angles O1-C4-C3 (121.14(3)°), O1-C4-C5 (115.56(3)°), C2-C3-C4 (116.53(3)°) and C4-C5-C9 (108.00(3)°) were narrowed, and the angle C4-C5-C6 was opened (111.50(3)°). Our thought about those synchronous angle deviances in (**a**) is that the hybrid resonance structure gives to C4=O1 group a hydroxylic character, as well as the intramolecular hydrogen bond O2-H2...O1 plays a similar role in the same way. Therefore, the expected value for this angle C3-C4-C5 is longer than related ones. The intramolecular hydrogen bond O2-H2...O1 also interferes in the valence angle geometry involving the hydroxyl group C10-OH2. Significant changes have been observed in adjacent angles to C10-OH2 bond from (**a**). Thereby, the approximation of the C10-OH2 group to C4=O1 one by mean of intramolecular H-bond displaced the C3-C10 bond in the direction of the delocalized hexacyclic system. Such displacement can be confirmed by the slightly short intramolecular O1…O2 distance (2.390(4) Å), when analyzing others benzophenones as clusianone and epiclusianone, without altering in the O2-C10-C3 and O2-C10-C11 angle values. Consequently, the angle C2-C3-C10 is relaxed (123.80(3)°), and the angle C4-C3-C10 (117.90(3)°) is closer than the respective average values. Following the same thought, the C10-OH2 group is pulled away from the aromatic ring, and considering the previous C3-C10 bond distorting centripetal to chelating delocalized cycle, the angle C10-C11-C16 is up deviated (123.55(4)°), whereas the respective opposed angle C10-C11-C12 is restricted (117.95(4)°). Likewise, a suitable change from 120° requested for phenyl angles is noted, with C12-C11-C16 angle measuring 118.45(4)°. Finally, a subtle release is view in the adjacent aromatic angle C11-C12-C13 (121.28(4)°) as consequence of C12-C11-C16 angle contraction.

The (**a**) unusual bond lengths C5-C6 (1.615(5) Å) and C1-C8 (1.556(5) Å) were also observed in clusianone (1.603 Å for C5-C6 and 1.555 Å for C1-C8) and in epiclusianone(1.610(7) Å for C5-C6 and 1.562(6) Å for C1-C8) and they have been caused by marked tension about the C-C bonds due to involved C-atoms to be highly substituted, likewise hindrance effects can be related to this geometrical feature.[17] The C-OH bond lengths in the aromatic ring are very similar, with values of 1.372(6) Å for O5-C15 and 1.365(5) Å for O6-C14, and these values consist with an expected ones. On the other hand, the three C=O bond lengths are larger than average query ones. The double bond O1=C4 is longer (1.281(4) Å) than expected one, which is a consequence of the electronic delocalization above discussed. The carbonylic double bonds O4=C9 (1.221(5) Å) and O3=C2 (1.239(4) Å) are also enlarged when looking at the similar entries returned by MOGUL search. In addition, the O3=C2 bond length

found in (**a**) is longer than that determined in epiclusianone (1.208(6) Å). Again, this fact is derived from electronic delocalization and resonance effects in the keto-enol moiety, indicating a possible contribution of C2-O3-H2/ C10=O2 form to (**a**) crystal structure.

Several aromatic C-C bond lengths shortened in (**a**), taken in account the common values in aromatic rings (1.39-1.40 Å). These variations are in the bonds C12-C13 (1.368(6) Å), C13-C14 (1.363(6) Å) and C15-C16 (1.368(6) Å). The shortening of certain aromatic C–C distances is reported in a series of related benzophenones.[30,31] Nevertheless, the aromatic distances found in (**a**) are in agreement with the range required for aromatic bonds, just as all aromatical C-C-C angles (mean of 120(4)°) coincided with the reference corners for the aromatic ring. In the same way, the C-C single and double bonds at the prenyl fragments present concordant distances in relation to similar prenylated compounds (mean distances of 1.311(4) Å for C=C, 1.500(4) Å for C_{sp^3}-C_{sp^2} and 1.549(5) Å for C_{sp^3}-C_{sp^3}).

The (**a**) prenyl C-C-C angles have been deviated from query mean values. The C4-C5-C19 angle connecting the bicyclic ring and the second prenyl group (including from the C19 to C23 atoms) is contracted (106.66(3)°), as well as the C5-C6-C18 angle that supports the fifth prenyl including from the C34 to C38 atoms (107.70(3)°). On the other hand, the valence angles C5-C6-C17 (111.44(3)°) and C6-C7-C24 (116.11(3)°), which binds the third prenyl unity including from the C24 to C28 atoms, are larger than the respective average measurement. These features are consequence of hindrance effect generated by the additional prenyl substituted at C18 atom. In tetraprenylated benzophenones clusianone[27] and epiclusianone,[17] the C18 methyl group is not sterically hindered as in the pentaprenylated benzophenone (**a**) due to the absence of the fifth bulky prenyl group. The C6-C5-C9 angle is fastened ((a) query value of 106.00(3)° against mean one of 109(4)°), indicating that the C9=O4 carbonyl group can be also moved away from steric domain of the second and fourth prenyl groups.

Looking the intermolecular geometry, it is verified that (**a**) exhibits one intermolecular hydrogen bond contributing to crystal packing (Figure 4a). The molecules are arranged in a stacking form, and the O6-H6…O3 hydrogen bond connects them along the [100] direction, forming an infinite one-dimensional chain. The packing is similar to that one observed to epiclusianone. The one exception is the epiclusianone packing is stabilized by non-classical hydrogen bonds (Figure 4b).

All hydrogen-bond contacts presents in the (**a**) networks are detailed in Table 2. The *para* hydroxyl group

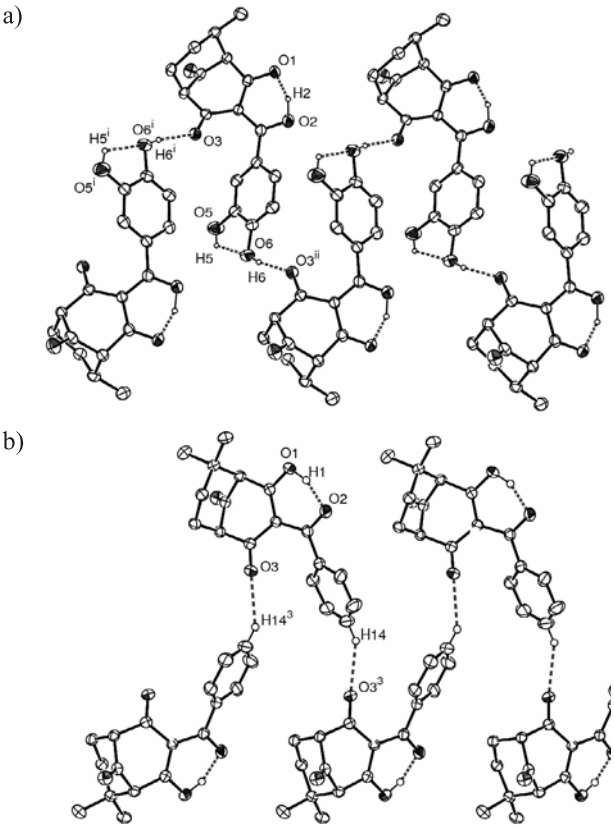

Figure 4. (a) Crystal packing view of (**a**) along the [100] direction. Double dotted lines represent hydrogen bonds. The C-H H-atoms and the last prenyl groups were omitted for clarity. Symmetry codes: (i) 1/2 + x, 3/2 - y, -z; (ii) –1/2 + x, 3/2 - y, -z; (3) 1/2 + x, 1/2 - y, 1/2 - z. (b) The Crystal packing view of epiclusianone[17] is shown in the same conditions.

in the aromatic ring, OH6, acts as an intermolecular H-bond donor to the carbonyl group C2=O3 and also as intramolecular H-bond acceptor from aromatic hydroxyl group OH5. These H-bonds contacts provide significant changes in the intramolecular geometry features. The O3-C2-C3 angle is 122.15(3)°, being that this corner is enclosed in relation to similar compounds analyzed in CSD. This feature is probably due to intermolecular H-bond O6-H6…O3 that slightly pulls the carbonyl group C2=O3 in the direction of the benzene ring from adjacent molecule in the lattice. This contact is also responsible by the insignificant O5 and O6 atoms deviations from the least squares plane through aromatic ring, taking the six ring C-atoms to calculate. The O6 deviation and the respective OH6-benzene dihedral angle H6-O6-C14-C13 are 0.051(6) Å and 0.07(5)°, respectively. These deviations are lower than expected for an aromatic OH group involved in an intermolecular H-bond. Such feature is due to electronic delocalization among OH6–Ph–C10-OH2 through resonance effect as above discussed, which become the 1,4-dihydroxyphenyl group almost completely planar. For O5 atom, the deviation from the least squares plane

and dihedral angle H5-O5-C15-C14 were found to be –0.049(6) Å and -0.6(5)°, respectively.

Table 2. Hydrogen-bonding length (Å) and angles (°) for (**a**). D and A mean hydrogen donor and acceptor, respectively

D-H...A	D-H	H...A	D...A	D-H...A
O2-H2...O1	1.04(6)	1.41(5)	2.390(4)	155(5)
O5-H5...O6	0.82	2.22	2.674(5)	115
O6-H6...O3*	0.82	1.98	2.790(4)	170

*Symmetry code: – 1/2 + x, 3/2 - y, -z.

The intramolecular O5-H5…O6 contact deviated three angles placed among the C and O atoms involved in this H-bond. The O6…H5 interaction contracted the O6-C14-C15 angle (115.91(4)°), and as consequence the O6-C14-C13 angle was enlarged (124.54(4)°. Likewise, the O5-C15-C14 corner is 120.09(4)°, an expanded value in reason to H-donation from OH5 group to OH6 one.

In addition, the spectroscopic data of (**a**) were also collected in order to check the concordance with that found in the literature. It presented infrared, ultraviolet and mass spectra data overlapped to literature ones. The IR spectrum exhibited typical absorption bands in 3450 (ν_{O-H}), 1730 ($\nu_{C=O}$ non-conjugated), 1670 ($\nu_{C=O}$ conjugated), 1600 ($\nu_{C=C}$ aromatic) cm^{-1}. The ^{1}H and ^{13}C NMR spectra, together with one and two-dimensional correlations and interactions (HMQC, HMBC and NOESY) allowed us to assign the structure of the benzophenone (**a**). The (**a**) structure at pyridine-d_5 solution was concluded to be the same tautomeric form from the solid state, which soon after was confirmed by comparation with data from literature.[1] However, an equilibrium switching the intramolecular hydrogen bond position between the O1 and O3 atoms, which act as hydrogen acceptors, was noted at pyridine-d_5 solution, and so two structures have been recognized. The keto-enol tautomer of (**a**) characterized in the present paper using X-ray diffraction analysis and NMR spectroscopic data in pyridine-d_5 solution differs from two forms assigned in $CDCl_3$ solution.[1]

The (**a**) UV absorption spectrum at methanol solution showed two main absorption bands at λ_{max} 230 and 281 nm. Stable bathochromic shifts at acid pH were observed in the absorptions above mentioned after anhydrous $AlCl_3$ adding, proving a characteristic behaviour from a chelating system and the boric acid adding indicated the presence of hydroxyl-groups at *o*-orientation.[32]

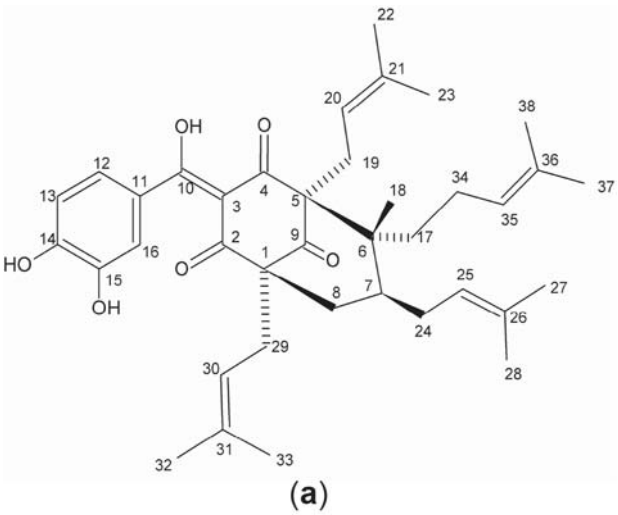

(a)

Scheme 1.

Conclusions

The crystal structure of (**a**) is entirely discussed in this paper, culminating in the precise identification of the intra and inter-molecular geometry. The most important structural variation observed in (**a**), characterized by the predominance of C10-O2-H2/C4=O1 tautomeric form in the (**a**) solid state in opposition to C10=O2/C4-O1-H1 tautomer in epiclusianone crystal structure, could be explained by the presence of aromatic OH6 group that possibly origins a further delocalized resonance structure along of OH6-Ph-C11-C10-O2. So, in (**a**) the O2-H2 bonding is covalent and O1…H2 is an intramolecular contact. The influence from OH6 group to molecular structure is strengthened through analysis of entire intra and intermolecular hydrogen bond geometry, which also pointed out the formation of a chelating delocalized hexacyclic system passing by O2-C10-C3-C4-O1-H2 atoms that influences several bond angles and lengths and torsional deviations in the whole (**a**) molecule. Furthermore, the differential localization of intramolecular H-bond between (**a**)/epiclusianone and clusianone can be in the stereochemistry of C7 atom.

The data published here must be primarily taken in account at the moment of structural assignments by NMR spectroscopic techniques performed in solution, once the X-ray diffraction experiment revealed also the presence of distinct tautomeric forms of (**a**) in the crystal structure and in $CDCl_3$ solution where structural assignments were previously performed by NMR method. In perspective, studies dealing to biological properties of (**a**) and epiclusianone, as protease inhibitory activity, will be carried out and structure-activity relationships will be stated in terms of their 3D structures.

Acknowledgments

The authors are grateful to CNPq (A.C.D and J.E.), CAPES (F.T.M.), and FAPEMIG (J.W.C.Jr) for research fellowships, FINEP (Proc.: 1110/06) and FAPEMIG (Proc.: EDT-3310/06) for financial support, and Instituto Rocasolano-CSIC, Spain, for the CSD license.

Supplementary Information

Spectroscopic and crystallographic data are available free of charge, at http://jbcs.sbq.org.br, as PDF file.

Supplementary crystallographic data sets for (**a**) are available through the Cambridge Structural Data Base, deposition number CCDC 643597. Copies of this information may be obtained free of charge from The Director, CCDC, 12 Union Road, Cambridge, CB2 1EZ, UK (fax: +44123-336-033; e-mail: deposit@ccdc.cam.ac.uk or http:www.ccdc.ac.uk)

References

1. Gustafson, K. R.; Blunt, J. W.; Munro, H. G. M.; Fuller, R. W.; McKee, C. T.; Cardellina, J. H.; McMahon, J. B.; Cragg, G. M.; Boyd, M. R.; *Tetrahedron* **1992**, *48*, 10093.
2. Williams, R. B.; Hoch, J.; Glass, T. E.; Evans, R.; Miller, J. S.; Wisse, J. H.; Kingston, D. G. I.; *Planta Med.* **2003**, *69*, 864.
3. Abe, F.; Nagafuji, S.; Okabe, H.; Akahane, H.; Muñiz, E. E.; Reyes, M. H.; Chilpa, R. R.; *Biol. Pharm. Bull.* **2004**, *27*, 141.
4. Pan, M. H.; Chang, W. L.; Lin-Shiau, S. Y.; Ho, C. T.; Lin, J. K.; *J. Agric. Food Chem.* **2001**, *49*, 1464.
5. Tanaka, T.; Kohno, H.; Shimada, R.; Kagami, S.; Yamaguchi, F.; Kataoka, S.; Ariga, T.; Murakami, A.; Koshimizu, K.; Ohigashi, H.; *Carcinogenesis* **2000**, *21*, 1183.
6. Yamaguchi, F.; Ariga, T.; Yoshimura, Y.; Nakazawa, H.; *J. Agric. Food Chem.* **2000**, *48*, 180.
7. Yamaguchi, F.; Saito, M.; Ariga, T.; Yoshimura, Y.; Nakazawa, H.; *J. Agric. Food Chem.* **2000**, *48*, 2320.
8. Waterman, P. G.; *Phytochemistry* **1986**, *25*, 3.
9. Delle Monache, G.; Botta, B.; de Mello, J. F.; Coelho, J. S. B.; Menichini, F.; *J. Nat. Prod.* **1984**, *47*, 620.
10. Corrêa, M. P.; *Dicionário das Plantas Úteis do Brasil e das Plantas Exóticas Cultivadas,* Imprensa Nacional: Rio de Janeiro, 1978.
11. Rubio, O. C.; Padron, A.; Castro, H. V.; Pizza, C.; Rastrelli, L.; *J. Nat. Prod.* **2001**, *64*, 973.
12. Gopalakrishnan, C.; Shankaranarayan, D.; Nazimudeen, S. K.; Kameswaran, L.; *Ind. J. Med. Res.* **1980**, *71*, 940.
13. Díaz-Carballo, D.; Seeber, S.; Strumberg, D.; Hilger, R. A.; *Int. J. Clin. Pharm. Th.* **2003**, *41*, 622.
14. Merza, J.; Aumond, M. C.; Rondeau, D.; Dumontet, V.; Le Ray, A. M.; Séraphin, D.; Richomme, P.; *Phytochemistry* **2004**, *65*, 2915.
15. Cruz, A. J.; Lemos, V. S.; dos Santos, M. H.; Nagem, T. J.; Cortes, S. F.; *Phytomedicine* **2006**, *13*, 442.
16. Piccinelli, A. L.; Cuesta-Rubio, O.; Chica, M. B.; Mahmood, N.; Pagano, B.; Pavone, M.; Barone, V.; Rastrelli, L.; *Tetrahedron* **2005**, *61*, 8206.
17. Santos, M. H.; Speziali, N. L.; Nagem, T. J.; Oliveira, T. T.; *Acta Crystallogr., Sect. C: Cryst. Struct. Commun.* **1998**, *54*, 1990.
18. Enraf-Nonius COLLECT. Nonius BV, Delft, The Netherlands, 1997-2000.
19. Otwinowski, Z.; Minor, W. In *Methods in Enzymology, 276*; Carter Jr., C. W.; Sweet, R. M., eds.; Academic Press: New York, 1997, ch. 15.
20. Sheldrick, G. M.; *SHELXS-97 Program for Crystal Structure Resolution*; University of Göttingen: Germany, 1997.
21. Sheldrick, G. M.; *SHELXL-97 Program for Crystal Structure Refinement*; University of Göttingen: Germany, 1997.
22. Farrugia, L. J.; *J. Appl. Crystallogr.* **1999**, *32*, 837.
23. Farrugia, L. J.; *J. Appl. Crystallogr.* **1997**, *30*, 565.
24. Bruno, I. J.; Cole, J. C.; Edgington, P. R.; Kessler, M. K.; Macrae, C. F.; McCabe, P.; Pearson, J.; Taylor, R.; *Acta Crystallogr., Sect. B: Struct. Sci*. **2002**, *58*, 389.
25. Bruno, I. J.; Cole, J. C.; Kessler, M.; Luo, J.; Motherwell, W. D. S.; Purkis, L. H.; Smith, B. R.; Taylor, R.; Cooper, R. I.; Harris, S. E.; Orpen, A. G.; *J. Chem. Inf. Comput. Sci.* **2004**, *4*, 2133.
26. Allen, F. H.; *Acta Crystallogr., Sect. B: Struct. Sci*. **2002**, *58*, 380.
27. McCandlish, L. E.; Hanson, J. C.; Stout, G. H.; *Acta Crystallogr., Sect. B: Struct. Sci*. **1976**, *32*, 1793.
28. Ettlinger, M. G.; Watson, K. J.; Jaroszewski, J. W.; *J. Am. Chem. Soc.* **1994**, *116*, 1557.
29. Korokolvas, A.; *Fundamentos de Farmacologia Molecular: Base para o Planejamento de Fármacos*, 2nd ed., Editora USP: São Paulo, 1974.
30. Doriguetto, A. C.; Martins, F. T.; Ellena, J. A.; Salloum, R.; dos Santos, M. H.; Moreira, M. E. C.; Schneedorf, J. M.; Nagem, T. J.; *Chem. Biodiversity* **2007**, *4*, 488.
31. Liebich, B. W.; *Acta Crystallogr., Sect. B: Struct. Sci*. **1979**, *35*, 1186.
32. Mabry, T. J.; Markham, K. R.; Thomas, M. B; *The Systematic Identification of Flavonoids,* Springer: Berlin, 1970.

Received: April 15, 2007
Web Release Date: December 10, 2007

FAPESP helped in meeting the publication costs of this article.

J. Braz. Chem. Soc., Vol. 18, No. 8, S1-S4, 2007.
Printed in Brazil - ©2007 Sociedade Brasileira de Química
0103 - 5053 $6.00+0.00

Natural Polyprenylated Benzophenones: Keto-Enol Tautomerism and Stereochemistry

Felipe T. Martins,[a] José W. Cruz Jr.,[a] Priscilla B. M. C. Derogis,[b] Marcelo H. dos Santos,[b] Márcia P. Veloso,[b] Javier Ellena[c] and Antônio C. Doriguetto*[,a]

[a]Laboratório de Cristalografia and [b]Laboratório de Fitoquímica e Química Medicinal, Departamento de Ciências Exatas, Universidade Federal de Alfenas, 37130-000 Alfenas-MG, Brazil

[c]Instituto de Física de São Carlos, Universidade de São Paulo, CP 369, 13560-970 São Carlos-SP, Brazil

Supplementary crystallographic data sets for (**a**) are available through the Cambridge Structural Data Base, deposition number CCDC 643597. Copies of this information may be obtained free of charge from The Director, CCDC, 12 Union Road, Cambridge, CB2 1EZ, UK (fax: +44123-336-033; e-mail: deposit@ccdc.cam.ac.uk or http:www.ccdc.ac.uk)

*Guttiferone A (**a**)*

Yellow crystalline solid, mp 120-123 °C (MeOH). $[\alpha]_D$ = +47.6° (c1.00,$CHCl_3$); IR (KBr) ν_{max}/cm^{-1}: 3450, 1730, 1670, 1600. UV (MeOH, 0.1 %) λ_{max}/nm: 228, 280. IE/MS *m/z* (%): 602 (1), 533 (22), 341 (42), 231 (34), 189 (9), 137 (26), 109 (11), 69 (100). The NMR data are as follows: ^{1}H NMR (400 MHz, pyridine-d_5) δ_H 7.87 (1H, *d*, *J* 2.1 Hz, H-12), 7.61 (1H, *dd*, *J* 2.1 and 8.3 Hz, H-16), 7.41 (1H, *d*, *J* 8.3 Hz, H-15), 5.76 (1H, *m*, H-20), 5.56 (1H, *m*, H-30), 5.20 (1H, *m*, H-25 and H-35), 3.04 (2H, *m*, H_2-24), 2.92 (2H, *m*, H_2-19 and H_2-29), 2.60 (2H, *m*, H_2-8b), 2.48 (2H, *d*, *J* 14.2 Hz, H_2-8a; *m*, H_2-8b), 2.33 (2H, *dd*, *J* 2.3 and 14.2 Hz, H_2-8a), 2.06 (1H, *m*, H-7), 2.06 (2H, *m*, H_2-34), 2.00 (2H, *m*, H_2-18), 1.79-1.59 (3H, *m*, H_3-22, H_3-23, H_3-27, H_3-28, H_3-32, H_3-33, H_3-37 and H_3-38), 1.52 (3H, *s*, H_3-17a), 1.01 (3H, *s*, H_3-17b); ^{13}C NMR (100 MHz, pyridine-d_5) δ_C 210.1 (C-9a), 201.7 (C-9b), 196.3 (C-10b), 195.9 (C-10a), 191.7 (C-2), 191.2 (C-4a), 191.1 (C-4b), 153.5 (C-14a), 147.2 (C-13b), 147.2 (C-13a), 143.1 (C-14b), 134.0 (C-31a), 133.8 (C-21a), 133.7 (C-21b), 133.4 (C-31b), 132.7 (C-26a), 132.1 (C-36a), 131.5 (C-26b), 131.2 (C-36b), 130.5 (C-11), 126.3 (CH-35a), 125.8 (CH-35b), 125.1 (CH-25a), 124.4 (CH-16a), 124.1 (CH-16b), 123.7 (CH-25b), 122.1 (CH-30), 121.8 (CH-20b), 121.0 (CH-20a), 119.0 (C-3), 117.5 (CH-12), 115.8 (CH-15a), 115.7 (CH-15b), 69.2 (C-5b), 62.9 (C-1b), 68.1 (C-5a), 61.2 (C–1a), 50.5 (C-6a), 49.8 (C-6b), 41.8 (CH_2-8b), 40.8 (CH-7b), 40.7 (CH-7a), 38.7 (CH_2-8a), 37.0 (CH_2-18b), 36.6 (CH_2-18a), 31.7 (CH_2-29a), 31.5 (CH_2-29b), 29.9 (CH_2-19), 26.5 (CH_2-24b), 26.4 (CH_2-24a), 26.3 (CH_3-27a), 26.3 (CH_3-27b), 26.1 (CH_3-23 and CH_3-33), 26.0 (CH_3-38a), 26.0 (CH_3-38b), 24.8 (CH_2-34b), 23.3 (CH_2-34a), 19.9 (CH_3-17a), 18.7 (CH_3-32), 18.6 (CH_3-28b), 18.5 (CH_3-28a), 18.5 (CH_3-22a), 18.4 (CH_3-22b), 18.2 (CH_3-37b), 17.9 (CH_3-37a), 16.5 (CH_3-17b).

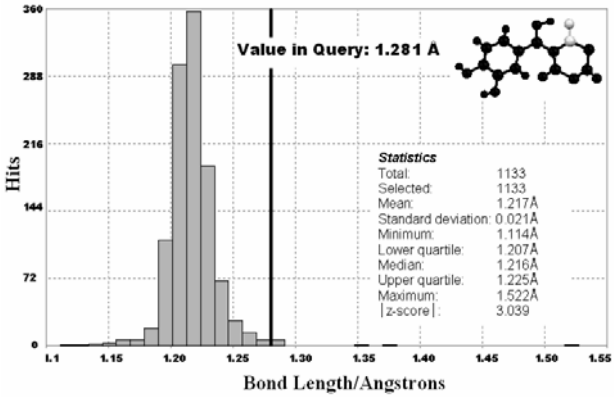

Figure S1. Histogram comparing the C4=O1 bond length with the C=O bond lengths in CSD entries containing structures similar to (**a**).

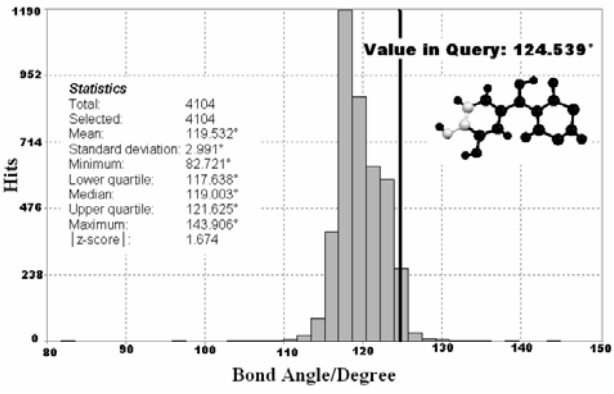

Figure S2. Histogram comparing the O6-C14–C13 bond angle with the O-C-C bond angles in CSD entries containing structures similar to (**a**).

*e-mail: doriguetto@unifal-mg.edu.br

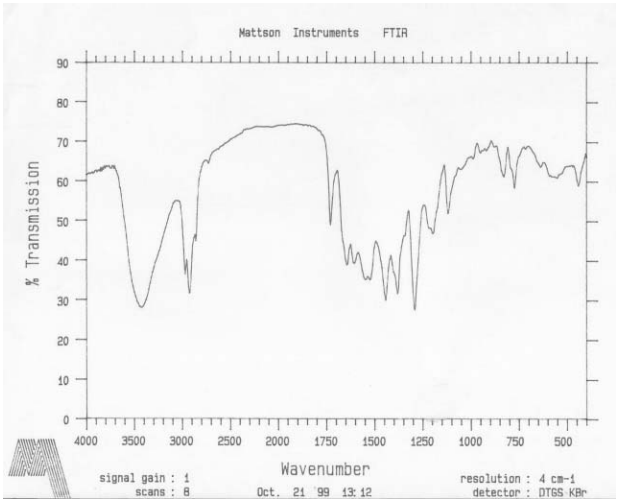

Figure S3. Infrared spectrum (KBr).

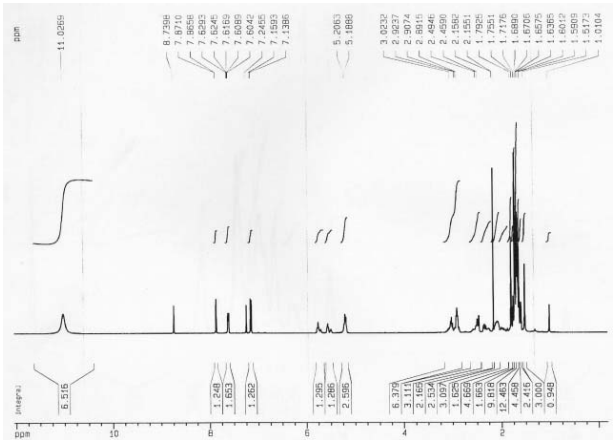

Figure S6. ^{1}H NMR spectrum (400 MHz, pyridine-d_5).

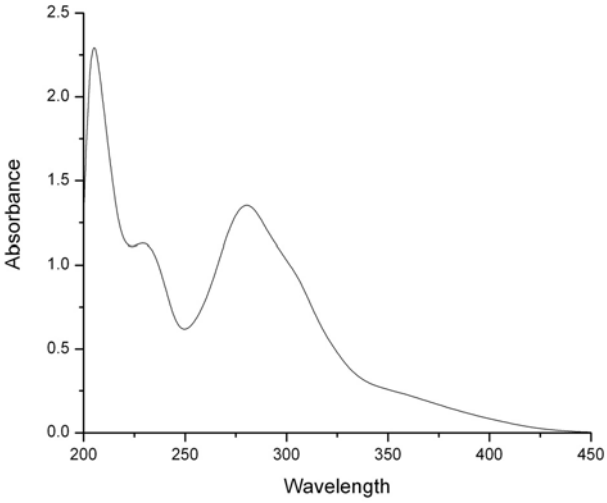

Figure S4. UV spectrum (MeOH, 0.1 %).

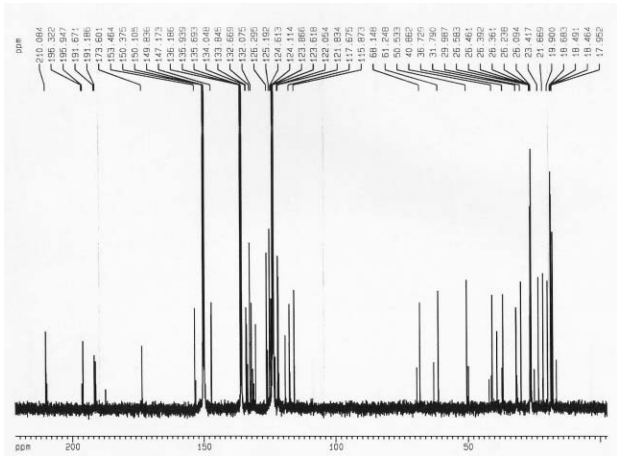

Figure S7. ^{13}C NMR spectrum (100 MHz, pyridine-d_5).

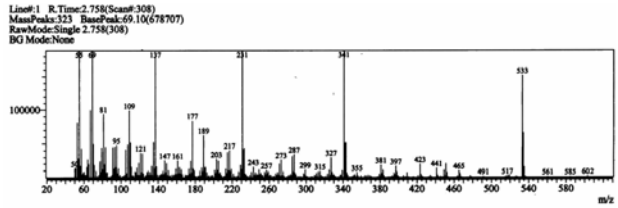

Figure S5. Electron impact mass spectrum.

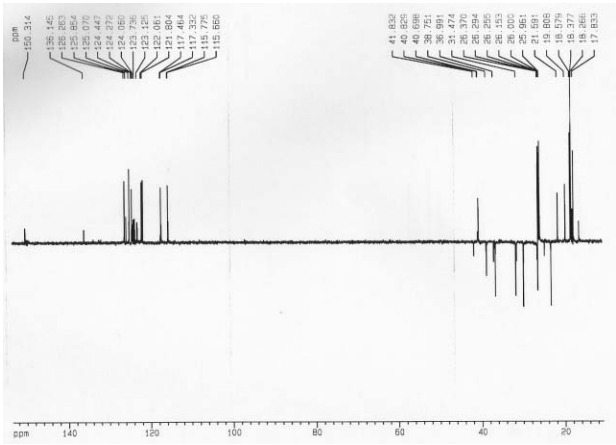

Figure S8. ^{13}C 135-DEPT NMR spectrum (100 MHz, pyridine-d_5).

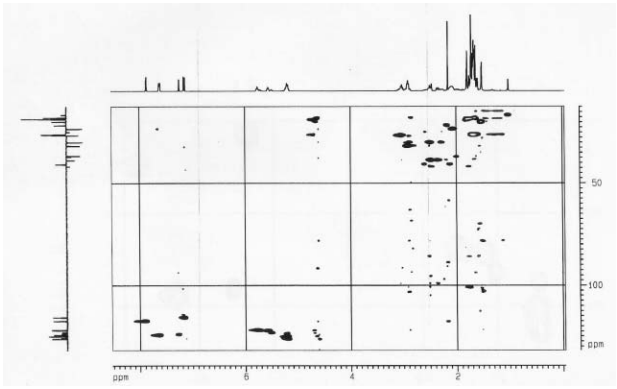

Figure S9. HMQC spectrum (400 and 100 MHz, pyridine-d_5).

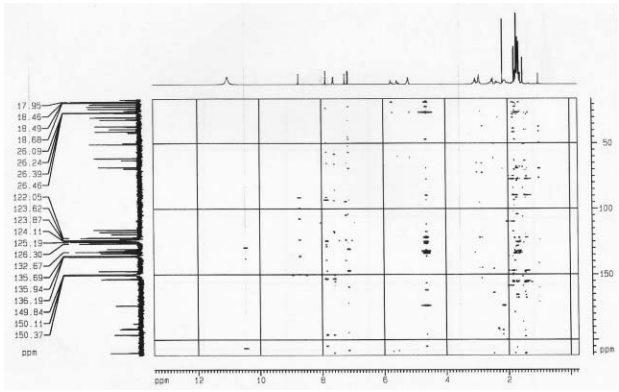

Figure S10. HMBC spectrum (400 and 100 MHz, pyridine-d_5).

Table S1. Bond lengths in Å for (**a**) determined by XRD (query value) and MOGUL intramolecular analysis

Bond	Hits	Mean	Query value
C1-C2	7	1.516 (2)	1.515 (5)
C2-C3	94	1.447 (3)	1.457 (5)
C3-C4	94	1.447 (3)	1.416 (5)
C4-C5	4	1.538 (2)	1.528 (5)
C5-C6	5	1.586 (2)	1.615 (5)
C6-C7	27	1.566 (4)	1.579 (5)
C7-C8	249	1.535 (2)	1.534 (5)
C1-C8	58	1.538 (2)	1.556 (5)
C1-C9	31	1.508 (4)	1.497 (5)
C1-C29	62	1.561 (5)	1.555 (5)
C3-C10	9	1.380 (1)	1.413 (5)
C5-C9	4	1.526 (2)	1.503 (5)
C5-C19	3	1.545 (5)	1.555 (5)
C6-C17	2438	1.537 (2)	1.526 (6)
C6-C18	18	1.550 (1)	1.551 (5)
C7-C24	22	1.545 (1)	1.538 (5)
C10-C11	44	1.481 (1)	1.469 (6)
C11-C12	10000	1.388 (2)	1.392 (6)
C11-C16	7743	1.390 (2)	1.392 (6)
C12-C13	10000	1.383 (2)	1.368 (6)
C13-C14	4105	1.391 (2)	1.363 (6)
C14-C15	216	1.395 (2)	1.389 (6)
C15-C16	2565	1.384 (2)	1.368 (6)
C18-C34	182	1.530 (4)	1.521 (6)
C19-C20	138	1.494 (3)	1.501(6)
C20-C21	334	1.315 (4)	1.309 (6)
C21-C22	1038	1.497 (3)	1.486 (7)
C21-C23	1038	1.497 (3)	1.513 (7)
C24-C25	160	1.497 (2)	1.485 (6)
C25-C26	334	1.315 (4)	1.316 (7)
C26-C27	1038	1.497 (3)	1.503 (7)
C26-C28	1038	1.497 (3)	1.514 (9)
C29-C30	138	1494 (3)	1.496 (7)
C30-C31	334	1.315 (4)	1.306 (8)
C31-C32	1038	1.497 (3)	1.535 (9)
C31-C33	1038	1.497 (3)	1.496 (9)
C34-C35	558	1.501 (3)	1.497 (7)
C35-C36	334	1.315 (4)	1.311 (7)
C36-C37	1038	1.497 (3)	1.468 (9)
C36-C38	1038	1.497 (3)	1.506 (8)
O1-C4	1133	1.217 (2)	1.281 (4)
O2-C10	155	1.329 (3)	1.297 (5)
O3-C2	1133	1.217 (2)	1.239 (4)
O4-C9	846	1.205 (2)	1.221 (5)
O5-C15	6759	1.362 (2)	1.372 (6)
O6-C14	6759	1.362 (2)	1.365 (5)

Table S2. Bond Angle (°) for (**a**) determined by XRD (query value) and MOGUL intramolecular analysis

Angle	Hits	Mean	Query value	Angle	Hits	Mean	Query value
C1-C2-C3	2	119 (2)	119.51 (3)	C11-C16-C15	85	119 (1)	119.66 (4)
C1-C8-C7	7	114 (1)	115.61 (3)	C12-C11-C16	2285	119 (2)	118.45 (4)
C1-C9-C5	3	114 (1)	114.83 (3)	C12-C13-C14	1329	120 (1)	119.97 (4)
C1-C2-C30	27	113 (2)	113.83 (3)	C13-C14-C15	169	119 (2)	119.55 (4)
C2-C1-C8	15	108 (2)	108.85 (3)	C14-C15-C16	218	119 (1)	120.99 (4)
C2-C1-C9	3	106 (4)	111.49 (3)	C17-C6-C18	12	108 (3)	107.78 (3)
C2-C1-C29	9	109 (2)	108.81 (3)	C18-C34-C35	150	113 (3)	112.96 (3)
C2-C3-C4	22	119 (1)	116.53 (3)	C19-C20-C21	68	128 (4)	128.24 (3)
C2-C3-C10	20	119 (2)	123.80 (3)	C20-C21-C22	668	122 (4)	124.23 (3)
C3-C4-C5	21	118 (3)	123.29 (3)	C20-C21-C23	668	122 (4)	121.62 (3)
C3-C10-C11	7	127 (1)	126.86 (3)	C22-C21-C23	519	114 (3)	114.14 (3)
C4-C3-C10	20	119 (2)	117.90 (3)	C24-C25-C26	24	128 (2)	130.66 (5)
C4-C5-C6	12	109 (3)	111.50 (3)	C25-C26-C27	668	122 (4)	121.57 (5)
C4-C5-C9	2	110 (1)	108.00 (3)	C25-C26-C28	668	122 (4)	123.12 (5)
C4-C5-C19	2	108 (1)	106.66 (3)	C27-C26-C28	519	114 (3)	115.31 (5)
C5-C6-C7	15	109 (3)	110.10 (3)	C29-C30-C31	68	128 (4)	127.79 (5)
C5-C6-C17	5	108 (1)	111.44 (3)	C30-C31-C32	668	122 (4)	121.71 (5)
C5-C6-C18	15	112 (2)	107.70 (3)	C30-C31-C33	668	122 (4)	125.55 (5)
C5-C19-C20	3	113 (1)	111.96 (3)	C32-C31-C33	519	114 (3)	112.68 (5)
C6-C5-C9	16	109 (4)	106.00 (3)	C34-C35-C36	109	127 (4)	128.95 (5)
C6-C5-C19	15	113 (2)	113.90 (3)	C35-C36-C37	668	122 (4)	122.33 (5)
C6-C7-C8	13	111 (2)	112.02 (3)	C35-C36-C38	668	122 (4)	120.71 (6)
C6-C7-C24	3	113 (1)	116.11 (3)	C37-C36-C38	519	114 (3)	116.90 (6)
C6-C18-C34	5	116 (2)	116.61 (3)	O1-C4-C3	94	124 (2)	121.14 (3)
C7-C6-C17	27	110 (2)	110.59 (3)	O1-C4-C5	4	120 (1)	115.56 (3)
C7-C6-C18	3	109 (1)	109.18 (3)	O2-C10-C3	8	119 (1)	119.22 (4)
C7-C24-C25	16	113 (3)	114.07 (3)	O2-C10-C11	44	113 (2)	113.92 (4)
C8-C1-C9	7	105 (2)	104.70 (3)	O3-C2-C1	7	119 (3)	118.15 (3)
C8-C1-C29	7	111 (1)	110.05 (3)	O3-C2-C3	94	124 (2)	122.15 (3)
C8-C7-C24	7	109 (2)	113.87 (3)	O4-C9-C1	31	121 (2)	122.72 (3)
C9-C1-C29	13	110 (3)	112.83 (3)	O4-C9-C5	4	122 (1)	122.07 (3)
C9-C5-C19	3	110 (1)	110.72 (3)	O5-C15-C14	432	118 (2)	120.09 (4)
C10-C11-C12	78	120 (2)	117.95 (4)	O5-C15-C16	2565	119 (3)	118.91 (4)
C10-C11-C16	10	119 (2)	123.55 (4)	O6-C14-C13	4104	119 (3)	124.54 (4)
C11-C12-C13	10000	120 (1)	121.28 (4)	O6-C14-C15	432	118 (2)	115.91 (4)